

Dynamics of the two-dimensional directed Ising model in the paramagnetic phase

C Godrèche¹ and M Pleimling²

¹Institut de Physique Théorique, CEA Saclay and CNRS
91191 Gif-sur-Yvette cedex, France

²Department of Physics, Virginia Polytechnic Institute and State University
Blacksburg, Virginia 24061-0435, USA

Abstract. We consider the non-conserved dynamics of the Ising model on the two-dimensional square lattice, where each spin is influenced preferentially by its East and North neighbours. The single-spin flip rates are such that the stationary state is Gibbsian with respect to the usual ferromagnetic Ising Hamiltonian. We show the existence, in the paramagnetic phase, of a dynamical transition between two regimes of violation of the fluctuation-dissipation theorem in the nonequilibrium stationary state: a regime of weak violation where the stationary fluctuation-dissipation ratio is finite, when the asymmetry parameter is less than a threshold value, and a regime of strong violation where this ratio vanishes asymptotically above the threshold. The present study suggests that this novel kind of dynamical transition in nonequilibrium stationary states, already found for the directed Ising chain and the spherical model with asymmetric dynamics, might be quite general. In contrast with the later models, the equal-time correlation function for the two-dimensional directed Ising model depends on the asymmetry.

1. Introduction

Physical systems which are defined by dynamical rules are not in general time reversible. Their stationary states can be arbitrarily difficult to determine and there is no general prescription to this end. Conversely, if the dynamics fulfills the condition of detailed balance with respect to the Hamiltonian describing the statics of the model, or, in other words, is reversible, then the system reaches an equilibrium state, described by statistical physics. Between these two cases lies an intermediate situation, where only the weaker constraint of global balance is imposed on the dynamics, in the sense that the stationary master equation of the process is globally satisfied by the same measure as at equilibrium. One may then wonder whether there exist models depending continuously on a parameter (or more generally on a set of parameters) such that the dynamics is either reversible or irreversible, in the later case with global balance being satisfied, according to the value of this parameter. If so, it is to be expected that the dynamical properties of these models will depend on whether the dynamics is reversible or not.

The directed Ising chain with non conserved dynamics [1, 2, 3] is a prototypical example of this kind of models. Directedness means that the flipping spin is unequally influenced by its two neighbours. For the linear chain, asymmetry of the dynamics and irreversibility go hand in hand: for any choice of the flipping rate function, invariant under spin reversal symmetry, the system relaxes to a stationary state described by the Boltzmann-Gibbs measure corresponding to the equilibrium Hamiltonian of the system, with the proviso that the parameters entering the rate function obey a condition fixing the temperature [3]. For special choices of these parameters the dynamics is reversible; restricting furthermore this choice leads to the solvable Glauber dynamics [4]. More generally, a one-parameter family of asymmetric dynamics can be shown to keep the exact solvability of the symmetric Glauber dynamics, allowing a detailed analysis of its dynamical features [2].

Such a Gibbsian asymmetric kinetic model, where the flipping spin is not equally influenced by its two neighbours, therefore provides a benchmark to study the physical consequences of irreversibility, in particular the properties of the resulting non-equilibrium stationary state. One of the most striking results is the existence of two regimes of violation of the fluctuation-dissipation theorem in the nonequilibrium stationary state. Indeed, the fluctuation-dissipation theorem [5], which gives a relation between response and correlation, is violated at stationarity as soon as the asymmetry parameter is non zero, because the dynamics becomes irreversible. Surprisingly this violation depends on the strength of the asymmetry: a dynamical transition is observed between a regime of weak violation with a finite asymptotic stationary fluctuation-dissipation ratio (the limit at large times of the ratio between the stationary response and correlation functions) when the asymmetry parameter is less than a threshold value, and a regime of strong violation where this ratio vanishes asymptotically above the threshold [2]. In the low temperature scaling regime, the asymptotic transient fluctuation-dissipation ratio depends on the strength of the asymmetry [2], and in particular vanishes at long times, as soon as the asymmetry is present, while in the absence of asymmetry it takes a universal value equal to $1/2$ [6, 7]. Another example where the same phenomena occur is the spherical model under asymmetric Langevin dynamics [8].

In the present work we address the situation of the directed Ising model on the two-dimensional square lattice. We consider the case where the flipping spin is more

influenced by its East and North neighbours than by its West and South ones. As shown in [1, 3] there exist rates such that, though the dynamics is asymmetric and irreversible, the stationary measure is still given by the Boltzmann-Gibbs distribution. Our aim is to investigate how the dynamical properties of the model are modified in the presence of the asymmetry and in particular whether the properties found in one dimension have a natural generalization in two dimensions. The present study is devoted to the paramagnetic phase: *our purpose is to investigate how the system, prepared in a disordered initial condition, relaxes to its stationary state, then fluctuates in this stationary state.* In a companion paper [9], we shall address the situation encountered at criticality and in the ferromagnetic phase.

We find that the two regimes of violation of the fluctuation-dissipation theorem uncovered for the linear chain are still present. This can be traced back, as was already the case of the chain, to the different behaviours of the linear and non linear relaxation rates: these two rates, initially equal in the absence of an asymmetry, take different values above a threshold value of the asymmetry parameter. We also find that the equal-time correlation function bears a dependence on the strength of the asymmetry, which reflects the fact that the dynamics of the two-dimensional Ising model is non linear, in contrast with the situation prevailing for the one-dimensional chain or the spherical model, where the correlation function is independent of the asymmetry parameter, in line with the fact that the dynamical equations are linear. However, this dependence of the equal-time correlation function on the strength of the asymmetry is very weak in the paramagnetic phase. At low temperature it becomes much stronger [9].

Let us finally point out an important difference between directed Ising models and other nonequilibrium models, such as the zero-range process [10], or the Ising chain evolving under Kawasaki dynamics and submitted to an external drive (the so-called KLS model [11]). These two models share, to a certain extent, similarities with the directed Ising models. Indeed, the stationary measure of the zero-range process, where particles hop from site to site on a graph with a rate only depending on the occupation of the departure site, is independent on whether the dynamics is reversible or not [12]. The same holds for the KLS model, in the sense that, with an appropriate choice of rates, the system relaxes towards a stationary state, the measure of which is identical to the equilibrium Boltzmann-Gibbs measure of the undriven chain [11, 13, 3]. However, in both examples, the dynamics is irreversible because there is an applied field on the system, which implies that there is transport of mass along the system, while for directed Ising models the asymmetry does not result from an externally applied field, hence *there is no macroscopic current transported in the system.*

The outline of the paper is as follows. Section 2 is devoted to the definition of the dynamical rules of our model. In section 3 we give a brief reminder of the main results of the study performed in [2] on the case of the linear chain, which will serve as a template for the study of the two-dimensional model. Sections 4 and 5 are the main parts of the present work. We first investigate the role of the asymmetry on the temporal evolution of the equal-time correlation function. We then demonstrate, by means of extensive numerical simulations, the existence of two regimes of violation of the fluctuation-dissipation theorem. We conclude by a discussion of our results.

2. Definition of the dynamical rules of the directed Ising model

In this section we give the definition of the dynamical rules of our model.

2.1. Expression of the rates with asymmetric dynamics

We consider a system of N Ising spins on a two-dimensional square lattice, with sites labeled $i = 1, \dots, N$. The energy of the configuration $\mathcal{C} = \{\sigma_1, \dots, \sigma_N\}$ reads

$$E(\mathcal{C}) = -J \sum_{(i,j)} \sigma_i \sigma_j, \quad (2.1)$$

where (i, j) are nearest neighbours and $J > 0$ is the coupling constant. From now on we will set $J = 1$ and $k_B = 1$ and denote the reduced coupling constant by $K = 1/T$.

At each instant of time, a spin, denoted by σ , is chosen at random and flipped with a rate $w(\sigma; \{\sigma_E, \sigma_N, \sigma_W, \sigma_S\})$, denoted for short by $w(\sigma; \{\sigma_j\})$, where $\{\sigma_j\} = \{\sigma_E, \sigma_N, \sigma_W, \sigma_S\}$ are the neighbours of the central spin σ , and E, N, W, S stand for East, North, etc.[‡] We choose the following form of the rate function:

$$\begin{aligned} w(\sigma; \{\sigma_j\}) = & \frac{\alpha}{2} \left[1 - \gamma \frac{1+V}{2} \sigma(\sigma_E + \sigma_N) - \gamma \frac{1-V}{2} \sigma(\sigma_W + \sigma_S) \right. \\ & \left. + \gamma^2 \frac{1+V}{2} \sigma_E \sigma_N + \gamma^2 \frac{1-V}{2} \sigma_W \sigma_S \right], \end{aligned} \quad (2.2)$$

where α fixes the scale of time, $\gamma = \tanh 2K$ and V is the asymmetry parameter, or velocity, which allows to interpolate between the symmetric case ($V = 0$) and the totally asymmetric ones ($V = \pm 1$). As commented in the next section, this expression of the rate function satisfies the condition of global balance, or otherwise stated, leads to a Gibbsian stationary measure with respect to the Hamiltonian (2.1). It represents one, among many, possible expression of a rate function, for the kinetic Ising model on the square lattice, possessing this property. This expression is invariant under up-down spin symmetry. In (2.2), for $V > 0$ (resp. $V < 0$) the couple (N, E) (resp. (S, W)) is more influential on the central spin than the other one.

The two particular cases of symmetric dynamics ($V = 0$), and completely asymmetric dynamics ($V = \pm 1$), deserve special attention. First, if $V = 0$, then the rate function

$$w(\sigma; \{\sigma_j\}) = \frac{\alpha}{2} \left[1 - \frac{\gamma}{2} \sigma(\sigma_E + \sigma_N + \sigma_W + \sigma_S) + \frac{\gamma^2}{2} (\sigma_E \sigma_N + \sigma_W \sigma_S) \right] \quad (2.3)$$

satisfies the condition of detailed balance. This form is different from the usual Glauber rate function (see (2.4) and (4.9) below). It does not possess all the symmetry of the former inasmuch as all neighbouring spins of the central spin do not play equivalent roles, i.e., cannot be interchanged (see also the comment at the end of this section). This can be demonstrated by looking at the values taken by $w(\sigma; \{\sigma_j\})$ according to the values of the local field $\sigma_E + \sigma_N + \sigma_W + \sigma_S$: if this sum is equal to ± 2 then all rates are the same. In contrast, if the sum vanishes then the rate function takes two different values, $\alpha(1 \pm \gamma^2)$, according to the configuration of the neighbours $\{\sigma_E, \sigma_N, \sigma_W, \sigma_S\}$: $\alpha(1 + \gamma^2)$ corresponds to $\{++--\}$ or $\{--++\}$, while $\alpha(1 - \gamma^2)$ corresponds to all other configurations. This is a manifestation of an anisotropy in the dynamics. For the Glauber case,

$$w(\sigma; \{\sigma_j\}) = \frac{\alpha}{2} [1 - \sigma \tanh K (\sigma_E + \sigma_N + \sigma_W + \sigma_S)], \quad (2.4)$$

[‡] The notation σ_N , where N stands for North, should not be confused with the notation for the spin with index N , size of the system.

if the sum vanishes, the rate function takes only one value, $\alpha/2$. Therefore, at zero temperature ($\gamma = 1$), all configurations such that the local field vanishes have a non-zero rate in the Glauber case, while in our model only the two configurations of neighbours $\{++--\}$ or $\{--++\}$ lead to a potential flip of the central spin.

The case with $V = 1$ corresponds to the totally asymmetric dynamics where the central spin σ is influenced by its East and North neighbours only. Then

$$w(\sigma; \{\sigma_j\}) = \frac{\alpha}{2} [1 - \gamma\sigma(\sigma_E + \sigma_N) + \gamma^2 \sigma_E \sigma_N]. \quad (2.5)$$

A similar expression, involving σ_W and σ_S , holds for $V = -1$:

$$w(\sigma; \{\sigma_j\}) = \frac{\alpha}{2} [1 - \gamma\sigma(\sigma_W + \sigma_S) + \gamma^2 \sigma_W \sigma_S]. \quad (2.6)$$

A remarkable fact about these expressions is that they are *unique*, up to the scale of time fixed by the choice of α : the rate function is uniquely determined by the condition of global balance, when only two neighbours, chosen among the four possible ones, are influential upon the central spin [1, 3].

As a final remark, let us point out that the rate function (2.2) is a linear combination of (2.5) and of (2.6), which makes its definition rather natural. Of course, one could define a more symmetrical rate function by taking a linear superposition of the expressions corresponding to the four couples NE (2.5), NW, SW (2.6), and SE. This choice would however imply the presence of more than one parameter in the rate function.

2.2. Derivation of the rate function (2.2)

With the aim of understanding the origin of the expression (2.2), we briefly come back on the main steps of the method used in [1, 3] to derive a set of constraints between the transition rates that need to be satisfied in order for the stationary state measure to be Gibbsian.

The dynamics consists in flipping the spin σ , chosen at random, with a rate $w(\bar{\mathcal{C}}|\mathcal{C})$, which is a more formal notation for $w(\sigma; \{\sigma_j\})$, corresponding to the transition between configurations \mathcal{C} and $\bar{\mathcal{C}} = \{\sigma_1, \dots, -\sigma, \dots, \sigma_N\}$. We choose periodic boundary conditions. At stationarity, the master equation expresses that losses are equal to gains, and reads

$$P(\mathcal{C}) \sum_{\bar{\mathcal{C}}} w(\bar{\mathcal{C}}|\mathcal{C}) = \sum_{\bar{\mathcal{C}}} w(\mathcal{C}|\bar{\mathcal{C}}) P(\bar{\mathcal{C}}), \quad (2.7)$$

where, by hypothesis, the weight of the configuration \mathcal{C} reads

$$P(\mathcal{C}) \propto e^{-E(\mathcal{C})/T}. \quad (2.8)$$

After division of both sides by the weight $P(\mathcal{C})$, eq. (2.7) can be rewritten as

$$\sum_{\bar{\mathcal{C}}} (w(\bar{\mathcal{C}}|\mathcal{C}) - w(\mathcal{C}|\bar{\mathcal{C}}) e^{-\Delta E/T}) = 0, \quad (2.9)$$

where the change in energy due to the flip reads

$$\Delta E = E(\bar{\mathcal{C}}) - E(\mathcal{C}) = 2\sigma(\sigma_E + \sigma_N + \sigma_W + \sigma_S). \quad (2.10)$$

While detailed balance consists in equating each individual term appearing on both sides of the stationary master equation (2.9), global balance means that this equation is satisfied as a whole. In other words (2.9) expresses the global balance condition on the rates, which are the unknown quantities of the latter. It leads to a

set of constraints on the rates which should be satisfied in order for the stationary state to be Gibbsian with Hamiltonian (2.1). (See [1, 3] for details.)

There are 32 (2^5) possible configurations of the group of spins $\{\sigma; \sigma_E, \sigma_N, \sigma_W, \sigma_S\}$ involved in the flipping of the central spin σ . Therefore, in the absence of any constraints on the dynamics, the most general form of the rate function $w(\sigma; \{\sigma_j\})$ takes 32 values, and thus depends on 32 parameters. We hereafter consider the simpler case where the rate function is invariant under spin reversal, which is possible in the absence of a magnetic field, i.e., we request the rate function to be invariant under the change of sign of $\sigma, \sigma_E, \sigma_N, \sigma_W, \sigma_S$:

$$w(-\sigma; \{-\sigma_E, -\sigma_N, -\sigma_W, -\sigma_S\}) = w(\sigma; \{\sigma_E, \sigma_N, \sigma_W, \sigma_S\}). \quad (2.11)$$

The number of possible values of the rate function is therefore halved and is equal to the number of different environments of the central spin σ , i.e., of configurations of its neighbours. There are 16 (2^4) such configurations, labelled by the index a . We denote the 16 rates with $\sigma = +1$ by w_a and the other 16 rates, corresponding to $\sigma = -1$, by \bar{w}_a :

$$w_a = w(\sigma = +1; \{\sigma_j\}_a), \quad \bar{w}_a = w(\sigma = -1; \{\sigma_j\}_a). \quad (2.12)$$

The latter are obtained from the former by the spin symmetry relation (2.11), yielding

$$\bar{w}_a = w_{17-a}, \quad (2.13)$$

(see Table 1). As a result, the number of independent parameters is decreased to 16.

Imposing now the global balance condition (2.9) yields, as shown in [1, 3], the set of constraints

$$\begin{aligned} e^{8K} w_1 - \bar{w}_1 &= 0, \\ w_6 - \bar{w}_6 &= 0, \\ e^{4K} w_2 - \bar{w}_2 + e^{4K} w_5 - \bar{w}_5 &= 0, \\ e^{4K} w_3 - \bar{w}_3 - (w_8 - e^{4K} \bar{w}_8) &= 0, \\ e^{4K} w_2 - \bar{w}_2 - (e^{4K} w_3 - \bar{w}_3) + \frac{2e^{4K}}{1 + e^{4K}} (w_7 - \bar{w}_7) &= 0, \\ e^{4K} w_2 - \bar{w}_2 + e^{4K} w_3 - \bar{w}_3 - \frac{2e^{4K}}{1 + e^{4K}} (w_4 - \bar{w}_4) &= 0. \end{aligned} \quad (2.14)$$

The rates constrained by the six conditions (2.14) now depend on ten independent parameters. Note that, in (2.14), the first two equations involve couples of rates related by detailed balance conditions, while the following ones are linear combinations of such couples.

This space of parameters can be further reduced by fixing the properties of the rate function under spatial symmetry. For the totally asymmetric dynamics where each spin sees only its East and North neighbours, the rate function is *uniquely* determined by the constraint equations (2.14) [1, 3], up to a scale of time, and is given by (2.5). Fixing this timescale by the choice $\alpha = 2 \cosh^2 2K$, allows to recast (2.5) into the compact form:

$$w(\sigma; \{\sigma_j\}) = e^{-2K\sigma(\sigma_E + \sigma_N)}. \quad (2.15)$$

This form appeared first in [14] without the factor 2 in the exponent, which amounts to replacing γ by $\tanh K$, and corresponds to a stationary state with the temperature halved. The uniqueness of this form was first shown in [1].

Table 1. List of local configurations and corresponding values of the rate function for the 2D square lattice. There are 16 possible rates w_a , with $\sigma = +1$, corresponding to the 16 possible configurations $\{\sigma_j\}$, labelled by a , of the four neighbours of the central spin, taken in the order: East, North, West, South. The 16 remaining rates \bar{w}_a , with $\sigma = -1$, are deduced from the former, due to the spin symmetry (see (2.13)).

a	$\sigma; \{\sigma_j\}$	w_a	$\sigma; \{\sigma_j\}$	\bar{w}_a
1	++;++++	w_1	-;++++	$\bar{w}_1 = w_{16}$
2	++;+++-	w_2	-;+++-	$\bar{w}_2 = w_{15}$
3	++;+-+	w_3	-;+-+	$\bar{w}_3 = w_{14}$
4	++;+--	w_4	-;+--	$\bar{w}_4 = w_{13}$
5	++;-++	w_5	-;-++	$\bar{w}_5 = w_{12}$
6	++;-+-	w_6	-;-+-	$\bar{w}_6 = w_{11}$
7	++;--+	w_7	-;--+	$\bar{w}_7 = w_{10}$
8	++;---	w_8	-;---	$\bar{w}_8 = w_9$
9	+;-++++	w_9	-;-++++	$\bar{w}_9 = w_8$
10	+;-+++-	w_{10}	-;-+++-	$\bar{w}_{10} = w_7$
11	+;-+-+	w_{11}	-;-+-+	$\bar{w}_{11} = w_6$
12	+;-+--	w_{12}	-;-+--	$\bar{w}_{12} = w_5$
13	+;- -++	w_{13}	-;- -++	$\bar{w}_{13} = w_4$
14	+;- -+-	w_{14}	-;- -+-	$\bar{w}_{14} = w_3$
15	+;- --+	w_{15}	-;- --+	$\bar{w}_{15} = w_2$
16	+;- ---	w_{16}	-;- ---	$\bar{w}_{16} = w_1$

As mentioned above, the rate function (2.3), which corresponds to the case where $V = 0$, does not possess the full permutation symmetry of the spins, i.e., is not a function of the local field $\sigma_E + \sigma_N + \sigma_W + \sigma_S$ only. It is nevertheless invariant under the spatial left-right and up-down symmetries, which, combined with the global balance condition (2.14), enforces the condition of detailed balance.

From now on we shall set $\alpha = 1$.

3. Reminder of the dynamics of the directed chain

The case of the linear chain will serve as a template for the study of the dynamics of the two-dimensional model. We therefore begin by a brief reminder of the main results of the study performed in [2].

The most general rate function, denoted by $w(\sigma_n; \{\sigma_j\})$, where σ_n is the flipping spin and $\{\sigma_j\}$ is a notation for the configuration of the neighbours $\{\sigma_{n-1}, \sigma_{n+1}\}$, invariant under spin reversal symmetry, depends on four independent parameters, i.e., takes four values according to the configuration chosen. Imposing global balance lowers the number of parameters to three. Imposing furthermore the solvability of the dynamical equations (i.e., their linearity) lowers this number to two: a global time-scale parameter α , as in (2.2), that we set equal to one, and an asymmetry parameter, which, in the particular case of one dimension, encodes entirely the role of irreversibility [3].

We thus obtain the following rate function [2]

$$w(\sigma_n; \{\sigma_j\}) = \frac{1}{2} \left[1 - \gamma \sigma_n \left(\frac{1+V}{2} \sigma_{n-1} + \frac{1-V}{2} \sigma_{n+1} \right) \right], \quad (3.1)$$

where V , the asymmetry parameter, has the meaning of a velocity, as can be seen, e.g., by following the motion of domain walls at zero temperature. This rate function interpolates between the totally symmetric model for $V = 0$, which is the usual Ising-Glauber model [4], and the totally asymmetric models for $V = \pm 1$. With this choice of rate function the temporal evolution of the observables defined hereafter obeys linear equations [2], as for the case of the Ising-Glauber model [4].

3.1. Observables

In order to characterize the relaxation of the system to its stationary state, amongst the various observables which can be monitored, we will focus only on a few of them, either in one or two dimensions. These are the magnetization,

$$M_n(t) = \langle \sigma_n(t) \rangle, \quad (3.2)$$

the equal-time correlation function,

$$C_n(t) = \langle \sigma_0(t) \sigma_n(t) \rangle, \quad (3.3)$$

and the two-time correlation function, where $s < t$,

$$C_n(s, t) = \langle \sigma_0(s) \sigma_n(t) \rangle. \quad (3.4)$$

We are also interested in the two-time response, which by translation invariance only depends on the difference $n - m$,

$$R_{n-m}(s, t) = \left. \frac{\delta M_n(t)}{\delta H_m(s)} \right|_{\{H=0\}}, \quad (3.5)$$

where H is an externally applied field, in reduced temperature units.

3.2. Symmetric dynamics

First, for symmetric dynamics ($V = 0$), i.e., for the Ising-Glauber model, we have the following results [4, 6].

At equilibrium, the characteristic scale of correlations is given by the correlation length ξ_{eq} . The latter is defined by the spatial decay of the spin-spin correlation function at equilibrium

$$C_{n,\text{eq}} = (\tanh K)^{|n|} = e^{-|n|/\xi_{\text{eq}}}. \quad (3.6)$$

On the other hand, the temporal decay of the equal-time correlation function to its equilibrium value behaves, according to [6], eq. (3.19), as

$$C_{n,\text{eq}} - C_n(t) \sim e^{-\alpha t}, \quad (3.7)$$

with

$$\alpha = \frac{2}{\tau_{\text{eq}}}, \quad \tau_{\text{eq}} = \frac{1}{1 - \gamma}, \quad (3.8)$$

where τ_{eq} , the equilibrium relaxation time, is the only characteristic time scale present in the theory. It is for example the time scale for the decay of the magnetization $M_n(t) = \langle \sigma_n(t) \rangle$. Let the initial magnetization be $M_n(0)$. Then, since all evolution

equations are linear in the symmetric case, the magnetization at time t is a discrete spatial convolution

$$M_n(t) = M_n(0) * G_n(t) = \sum_m M_{n-m}(0)G_m(t), \quad (3.9)$$

where $G_n(t)$, the magnetization at time t for a random initial condition, with the spin at the origin pointing upwards, that is to say the Green function for the magnetization [6], reads§

$$G_n(t) = e^{-t} I_n(\gamma t) \sim e^{-\alpha_G t}, \quad (3.10)$$

with the relaxation rate (inverse relaxation time)

$$\alpha_G = 1 - \gamma. \quad (3.11)$$

For an initially uniformly magnetized system, with $M_n(0) = M$, we have in particular

$$M_n(t) = M e^{-t/\tau_{\text{eq}}}. \quad (3.12)$$

It is easily shown that $G_n(t)$ is identical to the two-time correlation function,

$$C_n(0, t) = \langle \sigma_0(0) \sigma_n(t) \rangle, \quad (3.13)$$

which is the overlap between the configuration at time t and the totally disordered initial condition $\{\sigma_n(0)\}$.

The two-time equilibrium correlation and response functions decay exponentially with the relaxation rates α_C and α_R , both identical to α_G ,

$$C_{n,\text{eq}}(\tau) = \lim_{s \rightarrow \infty} C_n(s, s + \tau) \sim e^{-\alpha_C \tau}, \quad (3.14)$$

$$R_{n,\text{eq}}(\tau) = \lim_{s \rightarrow \infty} R_n(s, s + \tau) \sim e^{-\alpha_R \tau}. \quad (3.15)$$

The relationship between the two quantities is more precisely given by the fluctuation-dissipation theorem [5]

$$R_{n,\text{eq}}(\tau) = - \frac{dC_{n,\text{eq}}(\tau)}{d\tau}. \quad (3.16)$$

We will refer to α_C and α_G (or α_R) as the linear and non linear relaxation rates, respectively.

3.3. Asymmetric dynamics

For asymmetric dynamics ($V \neq 0$), we have the following results [2].

(i) The equal-time correlation function $C_n(t)$ is independent of the asymmetry. Hence (3.6) and (3.7) hold unchanged. This property, also shared by the spherical model under asymmetric Langevin dynamics [8], has its origin in the linearity of the dynamical equations.

(ii) We have

$$C_n(0, t) = G_n(t) \sim e^{-\alpha_G t}, \quad (3.17)$$

with a decay rate which varies continuously with V ,

$$\alpha_G = 1 - \gamma \sqrt{1 - V^2}. \quad (3.18)$$

§ I_n is the modified Bessel function.

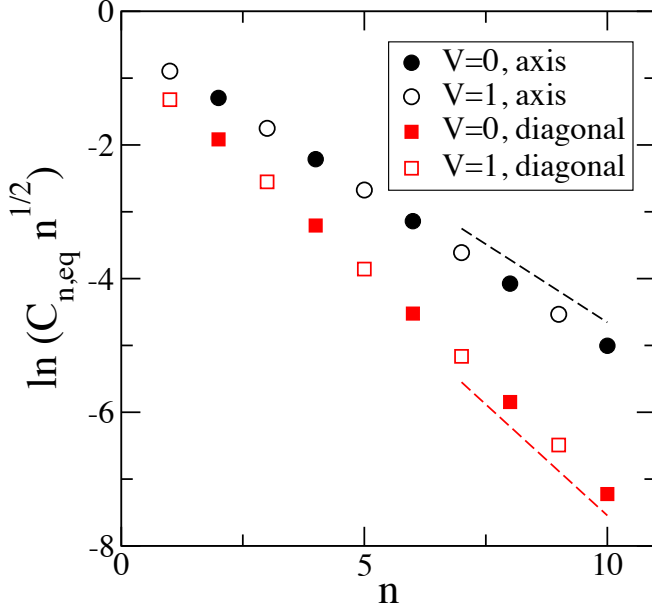


Figure 1. Stationary spatial correlation function of the two-dimensional model along the axes and diagonals, at $T = 3$, for $V = 0$ and $V = 1$. The inverse of the slopes yield estimates for the equilibrium correlation lengths in axial and diagonal directions. The dashed lines indicate the inverse of the exactly known values of ξ_{eq} given in equations (4.3) and (4.4). The system has been relaxed for $t = 1000$ time steps before measuring the correlation. The data result from averaging over 24 000 independent runs.

Hence, the larger the asymmetry, the faster the decay: the dynamics is accelerated by the asymmetry. The complete expression of the Green function is:

$$G_n(t) = e^{-t} \left(\frac{1+V}{1-V} \right)^{n/2} I_n(\gamma t \sqrt{1-V^2}). \quad (3.19)$$

It is thus invariant under the simultaneous sign changes of n and V . Conversely, for a fixed value of V , $G_n(t)$ is spatially asymmetric, as demonstrated by the expression of the time-independent ratio

$$\frac{G_n(t)}{G_{-n}(t)} = \left(\frac{1+V}{1-V} \right)^n. \quad (3.20)$$

We can thus define a length scale associated to this asymmetry by

$$e^{\pm 1/\xi_{\text{asym}}} = \sqrt{\frac{1+V}{1-V}}, \quad (3.21)$$

where the sign \pm corresponds respectively to the cases $V > 0$ and $V < 0$. This length, even in V , diverges for $V = 0$ as $\xi_{\text{asym}} \approx \pm 1/V$ and vanishes for $V = \pm 1$.

(iii) At stationarity, the two-time correlation function

$$C_{n,\text{stat}}(\tau) = \lim_{s \rightarrow \infty} C_n(s, s + \tau) \sim e^{-\alpha_C \tau}, \quad (3.22)$$

is exponentially decreasing with the decay rate

$$\alpha_C = \begin{cases} \alpha_1 = 1 - \gamma\sqrt{1 - V^2} = \alpha_G, & (V < V_c) \\ \alpha_2 = V\sqrt{1 - \gamma^2}, & (V > V_c). \end{cases} \quad (3.23)$$

The two decay rates α_1 and α_2 are equal at the critical velocity $V_c = \sqrt{1 - \gamma^2}$.

On the other hand, the stationary response function reads

$$R_{n,\text{stat}}(\tau) = \sqrt{1 - \gamma^2} G_n(\tau), \quad (3.24)$$

implying the equality of relaxation rates $\alpha_R = \alpha_G$.

From now on, unless otherwise stated, we shall focus on the correlation and response functions at coinciding points ($n = 0$).

(iv) As a consequence of the above, the fluctuation-dissipation theorem (3.16) no longer holds. Its violation can be quantified by the limit stationary fluctuation-dissipation ratio X_{stat} defined as [2]

$$X_{\text{stat}} = \lim_{\tau \rightarrow \infty} X_{\text{stat}}(\tau) = \lim_{\tau \rightarrow \infty} \frac{R_{0,\text{stat}}(\tau)}{-dC_{0,\text{stat}}(\tau)/d\tau}. \quad (3.25)$$

This ratio has the following behaviour:

- (a) For $V < V_c$, the relaxation rates of the two quantities are both equal to α_1 . It turns out that the sub-leading corrections to the exponential decay are also the same, with the consequence that the stationary fluctuation-dissipation ratio has the finite limit

$$X_{\text{stat}} = \frac{1 - \gamma/\sqrt{1 - V^2}}{1 - \gamma\sqrt{1 - V^2}}. \quad (3.26)$$

In particular, for $V = 0$, we have $X_{\text{stat}} \equiv X_{\text{eq}} = 1$, in accordance with (3.16).

- (b) For $V > V_c$, this ratio vanishes, because the relaxation rate of the response, $\alpha_R = \alpha_G = \alpha_1 = 1 - \gamma\sqrt{1 - V^2}$, is always larger than the relaxation rate of the correlation, $\alpha_C = \alpha_2 = V\sqrt{1 - \gamma^2}$.

In summary, if $V < V_c$, the stationary fluctuation-dissipation ratio has a finite limit at large time because the correlation and response functions have the same asymptotic exponential decay. For $V > V_c$ the correlation function decays more slowly and $X_{\text{stat}} = 0$.

This dynamical transition has a simple interpretation in terms of the two length scales present in the theory, namely the equilibrium correlation length ξ_{eq} and the asymmetry length scale ξ_{asym} . The condition $V < V_c$ corresponds to the condition $\xi_{\text{eq}} < \xi_{\text{asym}}$. The effect of the asymmetry becomes dominant when $\xi_{\text{eq}} > \xi_{\text{asym}}$. The transition occurs when the two length scales cross [2].

Remark

The limit *stationary* fluctuation-dissipation ratio defined in (3.25) is different from the limit ratio X_∞ encountered in the study of the transient regime of nonequilibrium systems (see, e.g., [15, 16]). Defining the fluctuation-dissipation ratio as [17]

$$X(s, t) = \frac{R_0(s, t)}{\partial C_0(s, t)/\partial s}, \quad (3.27)$$

its asymptotic limit for $\tau = t - s$ large, denoted as $X_{\text{as}}(s)$ [6], reads

$$X_{\text{as}}(s) = \lim_{\tau \rightarrow \infty} X(s, s + \tau) \equiv \lim_{t \rightarrow \infty} X(s, t), \quad (3.28)$$

whose limit at large waiting time s yields the limit *transient* fluctuation-dissipation ratio

$$X_\infty = \lim_{s \rightarrow \infty} X_{\text{as}}(s) = \lim_{s \rightarrow \infty} \lim_{t \rightarrow \infty} X(s, t). \quad (3.29)$$

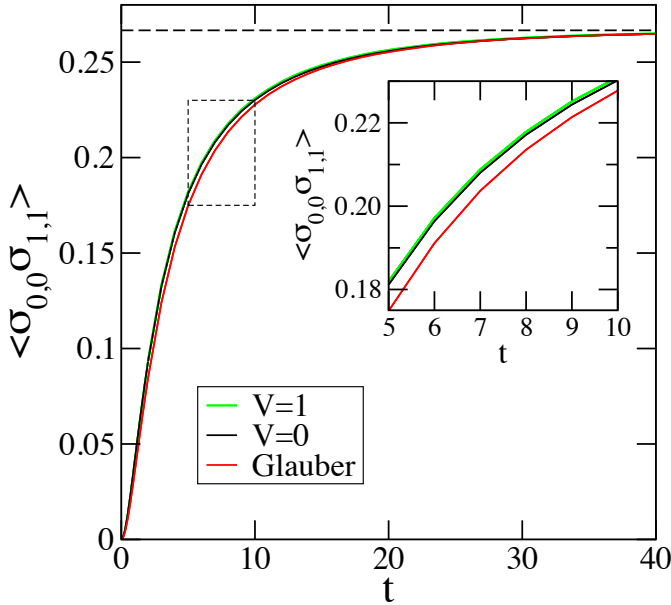


Figure 2. Growth of the North-East diagonal correlation function $\langle \sigma_{0,0}(t) \sigma_{1,1}(t) \rangle$ for $V = 0$, $V = 1$ and for the Glauber case at temperature $T = 3$. The horizontal line depicts the exact equilibrium value of the correlation at that temperature. The inset shows a blow-up of the region within the dashed box of the main figure and illustrates that the correlations grow faster for $V = 1$ than for $V = 0$, with the Glauber case yielding the slowest increase. The data result from averaging over two millions independent runs.

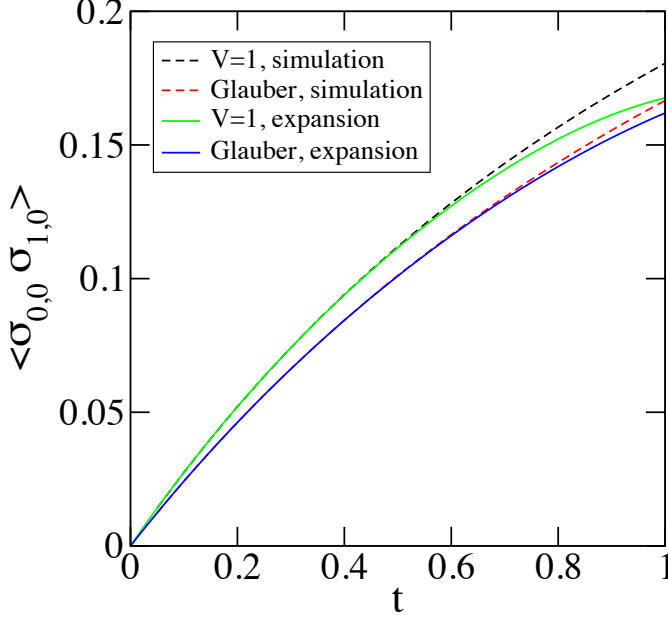


Figure 3. Comparison of the short-time expansions with simulations for the near neighbour axial correlation function $\langle \sigma_{0,0}(t) \sigma_{1,0}(t) \rangle$, both for the Glauber case and for our model with $V = 1$. (The corresponding curves for $V = 0$ are very close to those for $V = 1$.) Results are shown for the temperature $T = 3$.

4. Dynamics in the paramagnetic phase: equal-time correlations

We start our study of the two-dimensional directed Ising model on the square lattice by the investigation of the equal-time correlation function in the paramagnetic phase $T > T_c$.

We already know that its stationary value is independent of the asymmetry introduced by a finite velocity V , since the rate (2.2) leads to a Gibbsian stationary measure. The question is therefore whether, during its temporal evolution, this correlation function has, or has not, a dependence on the velocity. In one dimension, as recalled in section 3, the equal-time correlation is independent of the velocity and this is to be related to the fact that the dynamical equations are linear. In two dimensions the dynamics is non linear, and therefore, as can be expected, and as will be demonstrated below, the equal-time correlation bears a dependence on the velocity during its temporal evolution.

In practice, in order to elucidate the dynamics of our model, we relied on two approaches:

- (i) We performed extensive Monte Carlo simulations where we used the rate (2.2)

|| The critical temperature $T_c = 2/\ln(1 + \sqrt{2}) \approx 2.269185$ is such that $\sinh 2/T_c = 1$.

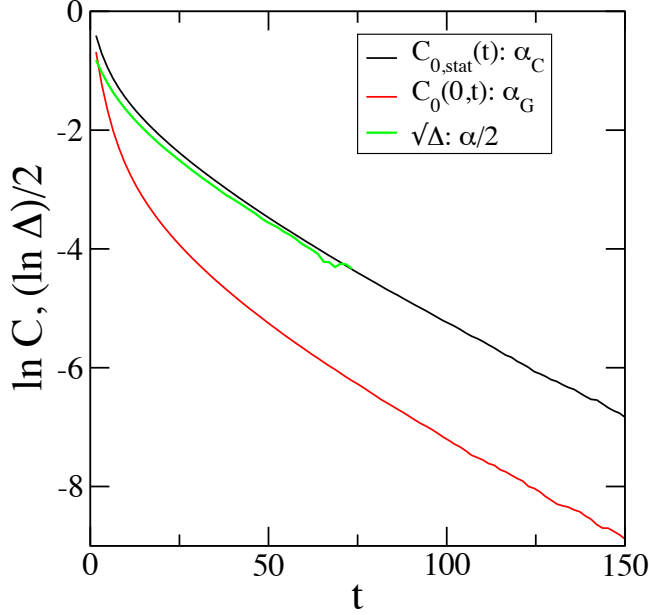


Figure 4. Comparison of the time dependence of (a): the stationary two-time correlation $C_{0,\text{stat}}(t)$ (5.1), (b): the overlap with the disordered initial condition $C_0(0,t)$ (5.2) and (c): the approach of the correlation function $\langle \sigma_{0,0}(t)\sigma_{1,1}(t) \rangle$ to its stationary value. The green line shows the square-root of $\Delta(t)$ (see (4.14)) in order to demonstrate that the exponential decays indicate the relationships $\alpha/2 \simeq \alpha_C \simeq \alpha_G$, see main text. All three cases correspond to $V = 0$ and temperature $T = 3$. For $C_{0,\text{stat}}(t)$ we averaged over 16 000 independent runs, whereas an average of much more runs has been done for the other two quantities: 660 000 runs for $C_0(0,t)$ and two millions run for $\Delta(t)$.

in order to decide whether a proposed flip of the spin σ_{m_i, n_i} , located at site i with integer coordinates (m_i, n_i) , should be accepted. Typically, we simulated systems composed of 300×300 spins. In all cases, a large number of independent runs were done and ensemble averages were determined (see the figure captions for details on the number of samples used in our study).

- (ii) We also carried out short-time expansions of the observables. The method used is straightforward, see, e.g., ref. [18].

4.1. Equilibrium equal-time correlation function

As mentioned above, at stationarity, the equal-time correlation function does not depend on V , and its asymptotic behaviour is known [19]. This therefore can be used as a test to validate our algorithm. In figure 1 we compare results obtained for $V = 0$ and $V = 1$ in two different directions, respectively along the x -axis, and along the

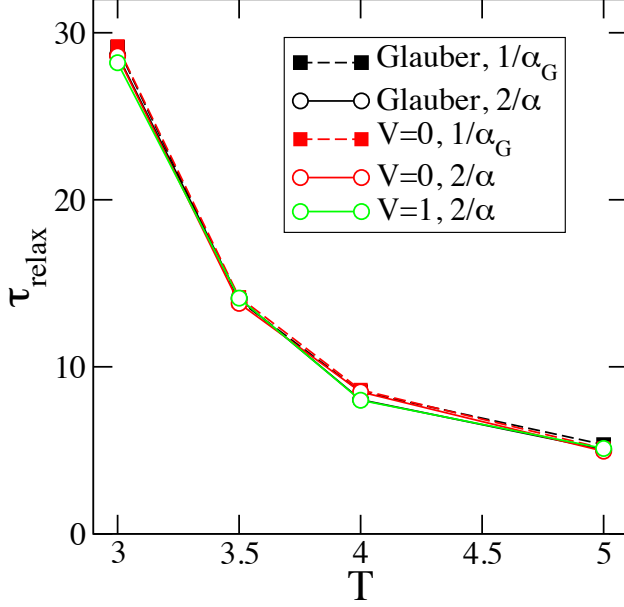


Figure 5. Comparison of the relaxation times obtained from the exponential decays of (4.14) and (5.2), for $V = 0$ and Glauber, and (4.14) for $V = 1$. We thereby use the relationship $\tau_{\text{relax}} = 1/\alpha_G$ for (5.2) and $\tau_{\text{relax}} = 2/\alpha$ for (4.14). Error bars are comparable to the sizes of the symbols.

North-East diagonal, with

$$\begin{aligned} C_{n,\text{eq}}(\text{axis}) &= \langle \sigma_{0,0} \sigma_{0,n} \rangle, \\ C_{n,\text{eq}}(\text{diag}) &= \langle \sigma_{0,0} \sigma_{n,n} \rangle, \end{aligned} \quad (4.1)$$

both at the same temperature $T = 3$. As expected, the results do not depend on the value of V . The asymptotic expression for the static correlation function for $T > T_c$ (see eqs. (2.43) and (2.46) in chapter XI of [19]) is of the form:

$$C_{n,\text{eq}} \sim e^{-|n|/\xi_{\text{eq}}} / n^{1/2}, \quad (4.2)$$

where the equilibrium correlation length ξ_{eq} depends on the angle. This behaviour is the two-dimensional counterpart of (3.6). Along the axes one has that

$$\xi_{\text{eq}}(\text{axis})^{-1} = \ln \frac{1-v}{v(1+v)}, \quad (4.3)$$

where $v = \tanh 1/T$, whereas along the diagonals

$$\xi_{\text{eq}}(\text{diag})^{-1} = 2 \ln \frac{1-v^2}{2v}. \quad (4.4)$$

Therefore, the inverse of the equilibrium correlation length is identical to the slope when plotting $\ln(C_{n,\text{eq}} n^{1/2})$ as a function of n , see figure 1. Our results obtained from simulations using the rate (2.2) agree perfectly with the exact results, indicated by the dashed lines in figure 1.

4.2. Relaxation of the equal-time correlation function

For $T > T_c$, when the system is initially out of equilibrium, the equal-time correlation function converges exponentially fast to its stationary (equilibrium) value, and this holds for any value of V .

Let us first focus on the near-neighbour North-East diagonal correlation function $\langle \sigma_{0,0}(t)\sigma_{1,1}(t) \rangle$, whose equilibrium expression is known exactly [19, 20] (see Appendix). Figure 2 depicts the behaviour of this function for $V = 0$ and $V = 1$. For comparison we also plot the same function obtained with the Glauber rate. The difference between the curves corresponding to $V = 0$ and $V = 1$ is of the order of 10^{-3} and therefore hardly visible on this figure. The existence of a difference can be demonstrated by looking at the short-time expansion of the correlation function. We could obtain such an expansion at order 4 in time t with little computing effort:

$$\langle \sigma_{0,0}(t)\sigma_{1,1}(t) \rangle \approx a_0 + a_1 t + \frac{a_2}{2!} t^2 + \frac{a_3}{3!} t^3 + \frac{a_4}{4!} t^4, \quad (4.5)$$

with $a_0 = 0$ since the initial condition is disordered, and

$$\begin{aligned} a_1 &= 0, & a_2 &= 2\gamma^2, & a_3 &= -2(4\gamma^2 + 3\gamma^4), \\ a_4 &= 24\gamma^2 + 60\gamma^4 + \frac{29}{2}\gamma^6 + \frac{7}{2}V^2\gamma^6. \end{aligned} \quad (4.6)$$

The role of the velocity is thus made apparent. Its importance increases as temperature is lowered, and vanishes at infinite temperature.

For comparison we give the corresponding short-time expansion for the Glauber case:

$$\begin{aligned} a_1 &= 0, & a_2 &= 8a^2, & a_3 &= -32a^2, \\ a_4 &= 4(24a^2 + 64a^4 - 160a^3b + 58a^2b^2 - 30ab^3 + 3b^4), \end{aligned} \quad (4.7)$$

where

$$a = \frac{\gamma(2 + \gamma^2)}{4(1 + \gamma^2)}, \quad b = \frac{\gamma^3}{4(1 + \gamma^2)} \quad (4.8)$$

are the parameters entering the Glauber rate (2.4), when it is written as an expansion on a basis of spin operators, as

$$\begin{aligned} w(\sigma; \{\sigma_j\}) &= \frac{1}{2} [1 - a(\sigma_E + \sigma_N + \sigma_W + \sigma_S) \\ &\quad + b(\sigma_E\sigma_N\sigma_W + \sigma_N\sigma_W\sigma_S + \sigma_W\sigma_S\sigma_E + \sigma_S\sigma_E\sigma_N)]. \end{aligned} \quad (4.9)$$

At high temperature, the expansions in γ of the coefficients (4.6), for the $V = 0$ case, and (4.9), for the Glauber case, match at leading order.

We also performed the short-time expansion of the North-West diagonal correlation function $\langle \sigma_{0,0}(t)\sigma_{-1,1}(t) \rangle$ in order to test the possible presence of an anisotropy in the temporal evolution of the correlation function, even when $V = 0$. We obtained:

$$\begin{aligned} a_1 &= 0, & a_2 &= 2\gamma^2, & a_3 &= -2(4\gamma^2 + 3\gamma^4), \\ a_4 &= 4(6\gamma^2 + 15\gamma^4 + 4\gamma^6). \end{aligned} \quad (4.10)$$

At this order this correlation function does not depend on V and the difference between the North-East and North-West correlations only appears in a_4 . It is equal

to $(7V^2 - 3)\gamma^6 t^4/2$, which changes sign when V increases. The dependence on V of the North-West correlation function only appears at order 5:

$$a_5 = -64\gamma^2 - 352(\gamma^4 + \gamma^6) + 2V^2\gamma^6 - \frac{1}{2}(99 + V^2)\gamma^8. \quad (4.11)$$

For completeness we also performed the short-time expansion of the axial near neighbour correlation function $\langle \sigma_{0,0}(t)\sigma_{1,0}(t) \rangle$ for our model:

$$\begin{aligned} a_1 &= \gamma, \quad a_2 = -(2\gamma + \gamma^3), \\ a_3 &= \frac{1}{2}(8\gamma + 18\gamma^3 + 3\gamma^5 + V^2\gamma^5), \\ a_4 &= -\frac{1}{4}(32\gamma + 168\gamma^3 + 156\gamma^5 + 24V^2\gamma^5 + 9\gamma^7 + 3V^2\gamma^7), \end{aligned} \quad (4.12)$$

and for the Glauber case:

$$\begin{aligned} a_1 &= 2a \quad a_2 = -4a \\ a_3 &= 8(a + 5a^3 - 5a^2b + ab^2), \\ a_4 &= -16(a + 15a^3 - 15a^2b + 5ab^2). \end{aligned} \quad (4.13)$$

Again, the two expansions match at high temperature. Figure 3 depicts a comparison between the two models at very short times.

As a conclusion, both the axial and diagonal near neighbour correlation functions depend on the velocity. The correlations grow faster for V larger. Let us emphasize that these differences, hardly visible for $T > T_c$, are on the contrary easily seen at low temperature [9]. The largest observed differences are nevertheless between the correlations for our model and for the Glauber case. Finally the presence of an anisotropy, even for $V = 0$, is revealed by the difference between the diagonal North-East and North-West correlations.

4.3. Approach of the correlation function to its stationary value

The approach of the near neighbour diagonal correlation function to its stationary value can be characterized by the decay rate α of the difference

$$\Delta(t) = \langle \sigma_{0,0}\sigma_{1,1} \rangle - \langle \sigma_{0,0}(t)\sigma_{1,1}(t) \rangle \sim e^{-\alpha t} \quad (4.14)$$

which is the counterpart of (3.7). As seen in the previous subsection, $\Delta(t)$ depends only weakly on V .

Anticipating on the sequel, in figure 4, we compared the rate α with the other characteristic relaxation rates appearing in the dynamics of the system, for the case $V = 0$. Inspired by the known behaviour of the linear chain, we compared the decay (4.14) to that of $C_{0,\text{stat}}(\tau)$ and $C_0(0, t)$, respectively given by (5.1) and (5.2) below. This comparison indicates that, for the case $V = 0$, $\alpha/2 \simeq \alpha_C = \alpha_G$, paralleling the property (3.8).

As a conclusion, in the paramagnetic phase, the equal-time correlation function of the two-dimensional directed Ising model behaves almost as its one-dimensional counterpart, since its dependence on the velocity is only very weak. While the decay rate α is weakly dependent on the velocity, this is not the case of the decay rates α_C and α_G , as analyzed in the next section.

5. Two-time observables

As discussed in section 3, the study of the one-dimensional directed Ising model revealed for a given temperature the existence of a critical velocity V_c that separates a regime of weak violation of the fluctuation-dissipation theorem for $V < V_c$ from one of strong violation for $V > V_c$. In the subsections below, following what was done in one dimension, we study different quantities that all should display signatures of this transition, provided it also takes place in the two-dimensional directed Ising model.

5.1. Determination of the different relaxation rates

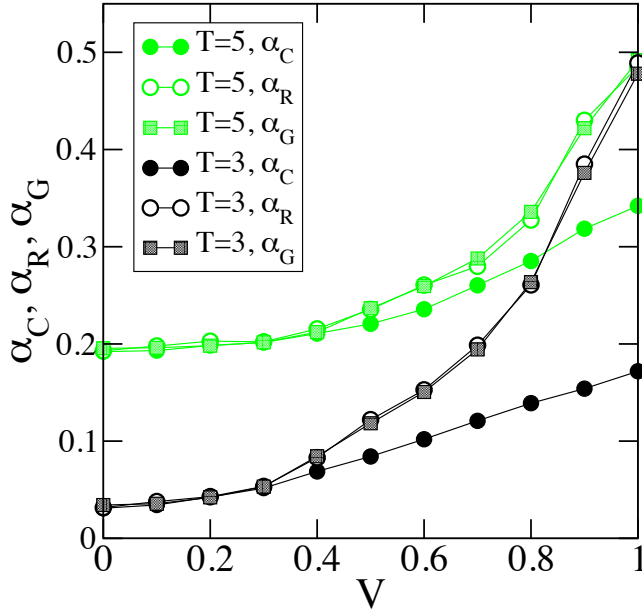


Figure 6. Decay exponents α_C , α_R , and α_G obtained from the stationary correlation $C_{0,\text{stat}}(\tau)$, the stationary integrated response function $\chi_{TRM}(\tau)$, and the correlation $C_0(0, t)$ far from stationarity. The condition $\alpha_R > \alpha_C$ for $V > V_c$ gives an estimate for the critical velocity shown in figure 7.

We start by investigating different relaxation rates which give a measure of the characteristic time scales. These relaxation rates are obtained from the exponential decay of various, stationary and non-stationary, correlation and response functions, whose definitions follow from the one-dimensional case and that we repeat here for convenience.

- (i) From the stationary two-time correlation,

$$C_{0,\text{stat}}(\tau) = \lim_{s \rightarrow \infty} \langle \sigma_{0,0}(s) \sigma_{0,0}(s + \tau) \rangle \sim e^{-\alpha_C \tau}, \quad (5.1)$$

we obtain the linear relaxation time $1/\alpha_G$, i.e., the decay time of stationary fluctuations. This quantity is the two-dimensional counterpart of (3.22).

- (ii) The overlap with the disordered initial condition yields the correlation

$$C_0(0, t) = \langle \sigma_{0,0}(0) \sigma_{0,0}(t) \rangle \sim e^{-\alpha_G t} \quad (5.2)$$

from which the nonlinear relaxation time $1/\alpha_G$ can be determined. This quantity is the two-dimensional counterpart of (3.13) and (3.17).

- (iii) Finally, the stationary response

$$R_{0,\text{stat}}(\tau) = \lim_{s \rightarrow \infty} R_0(s, s + \tau) \sim e^{-\alpha_R \tau} \quad (5.3)$$

is the counterpart of (3.15) and yields the additional relaxation time $1/\alpha_R$.

Figure 5 shows that the relaxation times obtained from the exponential decays of (4.14) and (5.2) are identical for Glauber dynamics and for the $V = 0$ case. Using the relationship $\tau_{\text{relax}} = 1/\alpha_G$ for (5.2) and $\tau_{\text{relax}} = 2/\alpha$ for (4.14), we find that the different quantities yield the same value for the relaxation time. The same τ_{relax} prevails for $V = 1$ when looking at the approach of the near neighbour diagonal correlation function to its stationary value.

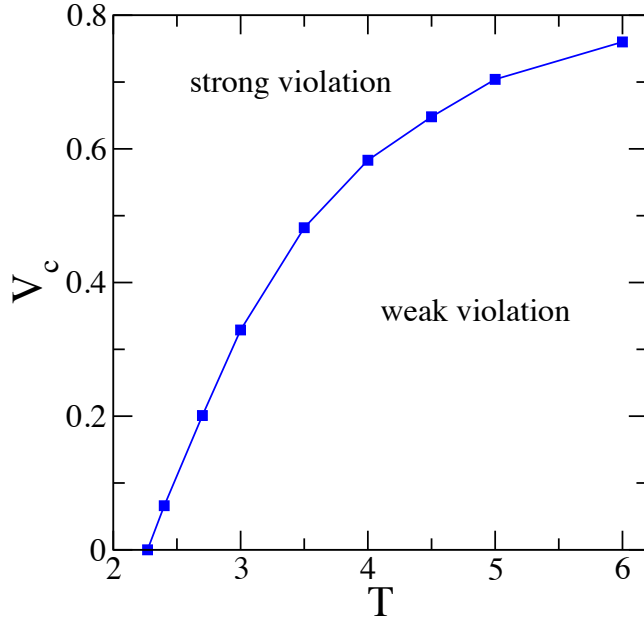


Figure 7. Critical value of the velocity V_c as a function of temperature. The blue squares are estimates for V_c obtained from the condition $\xi_{\text{asym}} = \xi_{\text{eq}}$, where ξ_{asym} is the length scale describing the asymmetry of the diagonal correlator $C_n(0, t)$, whereas ξ_{eq} is the equilibrium correlation length of the two-dimensional Ising model, see figure 9.

In figure 6 we show the dependence on V of the different rates α_C , α_G , and α_R for two different temperatures. We note that a scenario similar to that of the one-dimensional case prevails. On the one hand, the rate α_C is found to be equal to α_R for $V < V_c$, after which it varies approximately linearly with V . The rate α_G , on the other hand, is found to be equal to α_R . These later rates correspond both to quantities which measure the memory of a perturbation applied on the system far away in the past, and therefore we infer their strict equality. The velocity V_c , where the values of α_C and α_R start to differ, indicates the transition between the two dynamical regimes of violation of the fluctuation-dissipation theorem. This can be used to construct the $T - V_c$ phase diagram. In practice, however, it is rather difficult to reliably determine V_c in that way. We will see in the following that using the asymmetry correlation length provides a much more reliable way for the determination of the critical velocity, as shown in figure 7.

Remark

For convenience as well as in order to achieve better statistics, we do not determine directly the response $R_{0,\text{stat}}(\tau)$ (5.3), but instead we calculate time integrated quantities. We consider two different protocols, similar to those used routinely in studies of systems relaxing towards a steady state [21]. In the first protocol, a field with amplitude H_0 (in reduced temperature units) is applied between times s' and s after having reached the steady state. This yields the dimensionless time integrated susceptibility

$$\chi_{TRM}(s, s + \tau) = \int_{s'}^s du R_0(u, s + \tau), \quad (5.4)$$

which is proportional to the thermoremanent magnetization. At stationarity it decays with the same relaxation time as the response itself. In the second protocol, the field is applied continuously after time s , and the response is measured for times larger than s , yielding the dimensionless susceptibility

$$\chi_{ZFC}(s, s + \tau) = \int_s^{s+\tau} du R_0(u, s + \tau), \quad (5.5)$$

proportional to the zero field cooled magnetization. Practically, following [22], we apply at each site n a spatially random field $H_n = H_0 \epsilon_n$, where $\epsilon_n = \pm 1$, following one of the two protocols just discussed, and compute the staggered magnetization

$$M = \frac{1}{N} \left\langle \sum_n \epsilon_n \sigma_n \right\rangle, \quad (5.6)$$

from which the susceptibility $\chi = M/H_0$ is obtained. For the data obtained with the TRM protocol and discussed in the following, we applied the field for 100 time steps after having reached the steady state and then measured the susceptibility. We carefully checked that our results do not depend on the number of time steps during which the field has been switched on.

5.2. Determination of the asymmetry correlation length

In order to determine the asymmetry correlation length we proceed as for the one-dimensional case (see (3.20)) and make the ansatz

$$\frac{C_n(0, t)}{C_{-n}(0, t)} = e^{-2n/\xi_{\text{asym}}}, \quad (5.7)$$

where $C_n(0, t) = \langle \sigma_{0,0}(0) \sigma_{n,n}(t) \rangle$ is the overlap with the totally random initial state. Note that this assumes that the length ξ_{asym} is independent of time, which is confirmed by our simulations.

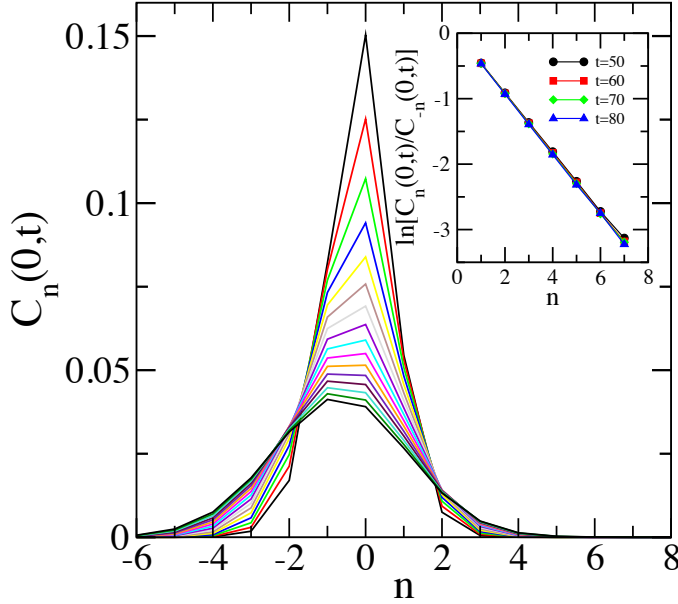


Figure 8. Correlation function $C_n(0, t)$ for $T = 2.4$ and $V = 0.1$. The value of t increases from 5 to 20 from top to bottom. The data result from averaging over 160 000 independent runs. Inset: The asymmetry length scale follows from the exponential change with n of the ratio $C_n(0, t)/C_{-n}(0, t)$.

The typical behavior of $C_n(0, t)$ is shown in figure 8 for $T = 2.4$ and $V = 0.1$, where we consider the correlation in the diagonal direction, i.e., $C_n(0, t) = \langle \sigma_{0,0}(0) \sigma_{n,n}(t) \rangle$. The expected asymmetry is very notable. Plotting the ratio (5.7) as a function of n in a log-log plot, see the inset of figure 8, then allows to determine a value for ξ_{asym} from the slope. Results from this procedure are shown in figure 9. This asymmetry correlation length can then be compared to the equilibrium correlation length ξ_{eq} (see (4.4) and the dashed lines in the figure). This allows to determine the critical velocity V_c , which is obtained by the condition $\xi_{\text{asym}} = \xi_{\text{eq}}$. The critical line $V_c(T)$ obtained in this way, as depicted in figure 7, is in fair agreement, at least for smaller values of T , with the line obtained from the relaxation times. In fact, using ξ_{asym} yields a more precise determination of V_c , via the intersection of the two lines ξ_{asym} and ξ_{eq} .

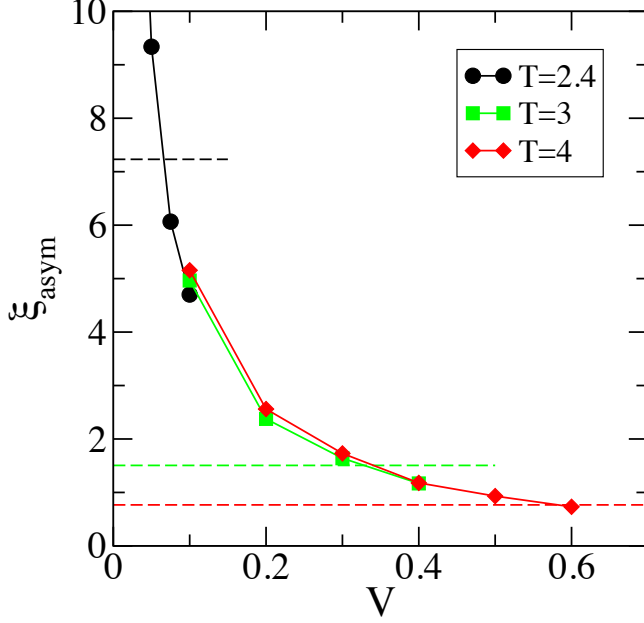


Figure 9. Asymmetry length scale ξ_{asym} as a function of V for three different temperatures. The dashed lines indicate the equilibrium correlation lengths of the two-dimensional Ising model at the different temperatures. The boundary between the weak and strong violation regimes is obtained when these two length scales coincide: $\xi_{\text{asym}} = \xi_{\text{eq}}$.

5.3. Fluctuation-dissipation ratio at stationarity

We close with a discussion of the fluctuation-dissipation ratio at stationarity. As discussed previously for the one-dimensional case, the violation of the fluctuation-dissipation theorem in the directed system can show up in two different ways. Indeed, for $V < V_c$ the limit fluctuation-dissipation ratio X_{stat} is expected to be larger than zero but smaller than the equilibrium value $X_{\text{eq}} = 1$. This regime corresponds to a weak violation of the fluctuation-dissipation theorem [2]. In contrast, for $V > V_c$, one should be in the regime of strong violation of the fluctuation-dissipation theorem, characterized by $X_{\text{stat}} = 0$.

In figure 10 the stationary integrated susceptibilities are plotted against the stationary autocorrelation $C_{0,\text{stat}}$ for $T = 3$. Figure 10a shows the zero-field cooled susceptibility χ_{ZFC} as a function of $C_{0,\text{stat}}$. This time integrated response increases with $\tau = t - s$. At the same time, the autocorrelation decreases with τ . Inspection of the curves $\chi_{ZFC}(C_{0,\text{stat}})$ indeed reveals that different behaviors are encountered for small and high velocities. For small values of V , χ_{ZFC} exhibits a finite slope when $C_{0,\text{stat}}$ is small, indicating the weak violation of the fluctuation-dissipation theorem. For large values of V , however, χ_{ZFC} has zero slope when $C_{0,\text{stat}}$ is small, which is the signature of the strong violation of the fluctuation-dissipation theorem.

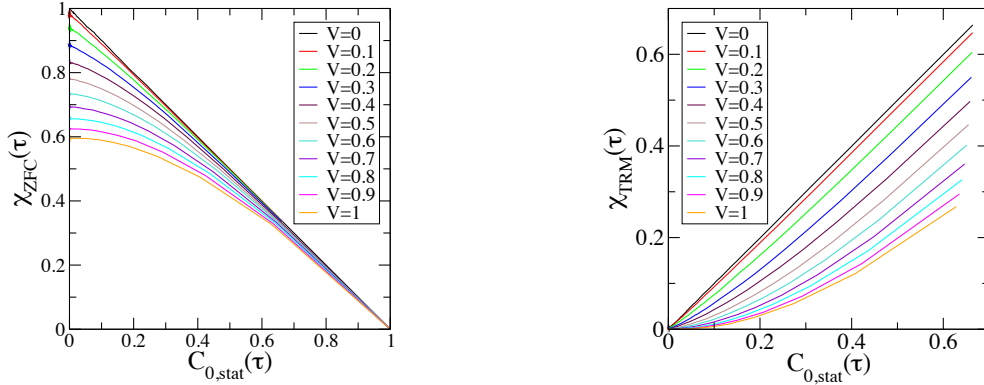


Figure 10. Stationary integrated response functions plotted against the stationary correlation at the temperature $T = 3$ for different velocities V . The system is relaxed for $s = 1\,000$ MCS before computing the quantities as a function of $\tau = t - s$. We carefully checked that we are indeed at stationarity, i.e., that the data only depend on the time difference τ . For the correlation function the data result from averaging over 1 000 independent runs. For the response function we average over typically 100 000 runs. Left panel: zero-field cooled susceptibility, right panel: thermoremanent susceptibility.

The limit stationary fluctuation-dissipation ratio X_{stat} is best extracted from the thermoremanent susceptibility. The ratio of the decaying susceptibility $\chi_{\text{TRM}}(\tau)$ to the correlation $C_{0,\text{stat}}(\tau)$ then yields X_{stat} for τ large, see figure 10b. In figure 11 we show the result of this analysis for three different velocities. For $V = 0$, $C_{0,\text{stat}}$ and χ_{TRM} are identical, in agreement with the fluctuation-dissipation theorem. For $V < V_c$, see the curves for $V = 0.2$, χ_{TRM} and $C_{0,\text{stat}}$ are no longer identical. Still, they decay with the same decay constant $\alpha_R = \alpha_C$, yielding, after an early-time regime, parallel lines in a log-log plot and a value for X_{stat} that is between 0 and 1. Finally, for $V > V_c$, see the curves for $V = 0.5$, $\alpha_R \neq \alpha_C$, and the ratio of χ_{TRM} and $C_{0,\text{stat}}$ goes to zero for large τ . Using the thermoremanent magnetization therefore provides us with a straightforward way to determine the limit fluctuation-dissipation ratio X_{stat} . The result of this procedure, shown in figure 12, indeed reveals the two different dynamical regimes.

6. Conclusion

In the present work we have pursued the investigation of the role of spatial asymmetry and irreversibility on the dynamics of spin systems, by considering the two-dimensional ferromagnetic Ising model on the square lattice with asymmetric dynamics. This line of research, initiated in [1], was followed by several works [2, 3, 8]. In particular ref. [2] is devoted to the case of the linear Ising chain with asymmetrical dynamics, while ref. [8] is devoted to the spherical model with asymmetric linear Langevin dynamics.

The outcomes of the present study turn out to share many common features with those of [2, 8]. Indeed, we show the existence of two regimes of violation of the fluctuation-dissipation theorem in the nonequilibrium stationary state: when the

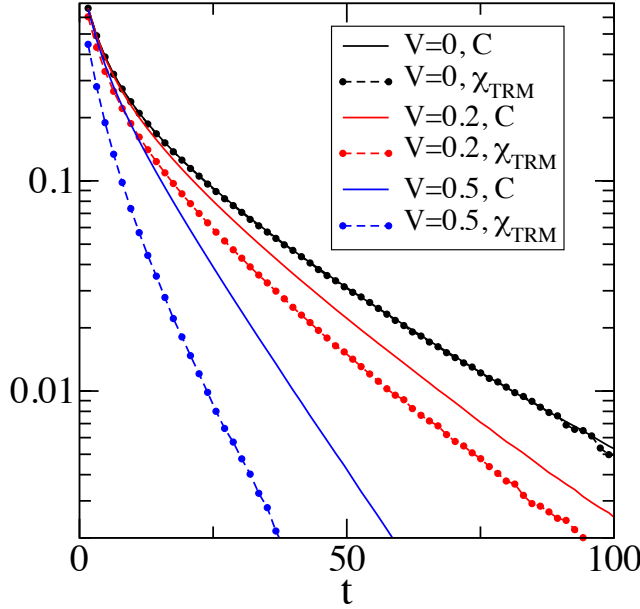


Figure 11. The correlation and the stationary thermoremanent magnetization for $T = 3$ and three different velocities: $V = 0$, $V = 0.2 < V_c$ and $V = 0.5 > V_c$, where $V_c \approx 0.34$ (see figure 9). For the computation of the stationary thermoremanent magnetization, a magnetic field of strength $h_0 = 0.05$ has been switched on for 100 time steps after having reached stationarity. The number of independent realizations are the same as in figure 10.

asymmetry parameter is less than a threshold value, there is weak violation of the fluctuation-dissipation theorem, with a finite asymptotic fluctuation-dissipation ratio, whereas this ratio vanishes above the threshold. The present results suggest that this novel kind of dynamical transition in nonequilibrium stationary states might be quite general.

While for the two models mentioned above, the directed Ising chain [2] and the ferromagnetic spherical model with asymmetric linear Langevin dynamics [8], the equal-time spin-spin correlation function does not feel the presence of the asymmetry in the dynamics, for the two-dimensional Ising case studied in the present work, this correlation function bears a dependence on the asymmetry. For the two former models the dynamics obeys linear equations, while for the model studied in the present work this no longer holds.

As was already the case for the linear chain, one of the consequences of the introduction of an asymmetry in the dynamics is the acceleration of the relaxation process towards stationarity. This can be seen for example on figure 6, where the relaxation rates, either linear or non linear, increase drastically with the asymmetry parameter V .

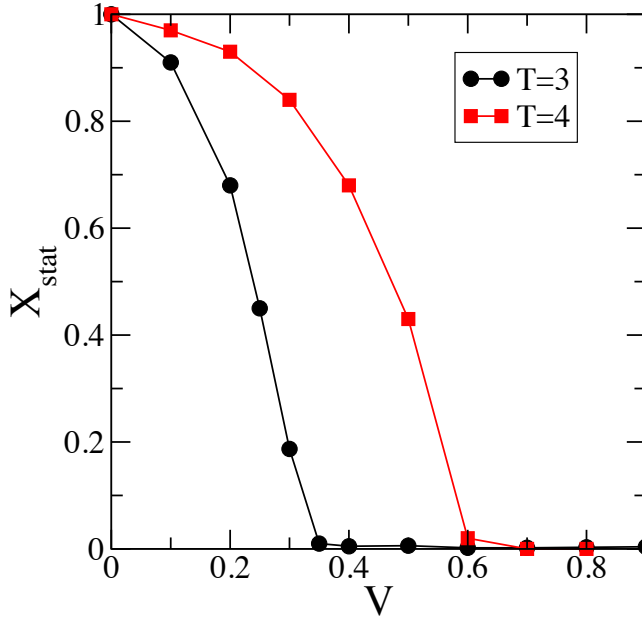


Figure 12. The stationary limit fluctuation-dissipation ratio as a function of velocity V for two different temperatures. These data are obtained from comparing the stationary integrated response function with the stationary correlation, see figure 11 for an example.

Some recent papers discuss how, for Markovian systems, the convergence towards the equilibrium Boltzmann-Gibbs distribution is accelerated by choosing dynamical rates violating detailed balance but fulfilling the condition of global balance [23, 24, 25, 26, 27, 28, 29]. There is therefore a conceptual overlap between those references and our work as well as the previous references [1, 2, 3, 8], but the former are more interested in algorithmic issues, while in our work as well as in [1, 2, 8, 3] the concern is oriented towards the role of irreversibility on the physical properties of the models. It would nevertheless be interesting to deepen the connections between the two topics.

In a companion paper, we shall address the situation encountered at criticality and in the ferromagnetic phase of the two-dimensional Ising model with asymmetric dynamics.

Acknowledgments

We wish to thank J-M Luck for fruitful discussions and M Henkel for his interest at an early stage of the present study. MP acknowledges financial support by the US National Science Foundation through grant DMR-1205309.

Appendix A. Equilibrium properties of the two-dimensional Ising model

In this appendix we recall some classical results on the near-neighbour correlation functions of the equilibrium Ising model on the square lattice used in the bulk of the paper (see e.g. [19, 20]). Let

$$k_{>} = \sinh^2 2/T = k_{<}^{-1}. \quad (\text{A.1})$$

Then, along the x -axis:

- for $T < T_c$,

$$\langle \sigma_{0,0} \sigma_{0,1} \rangle = \sqrt{1 + k_{<}} \left(\frac{1}{2} + \frac{1 - k_{<}}{\pi} K(k_{<}^2) \right), \quad (\text{A.2})$$

- for $T > T_c$:

$$\langle \sigma_{0,0} \sigma_{0,1} \rangle = \sqrt{\frac{1 + k_{>}}{k_{>}}} \left(\frac{1}{2} + \frac{k_{>} - 1}{\pi} K(k_{>}^2) \right). \quad (\text{A.3})$$

Along the diagonal:

- for $T < T_c$,

$$\langle \sigma_{0,0} \sigma_{1,1} \rangle = \frac{2}{\pi} E(k_{<}^2), \quad (\text{A.4})$$

- for $T > T_c$:

$$\langle \sigma_{0,0} \sigma_{1,1} \rangle = \frac{2}{\pi k_{>}} (E(k_{>}^2) + (k_{>}^2 - 1) K(k_{>}^2)). \quad (\text{A.5})$$

In these expressions

$$K(z) = \int_0^{\pi/2} dx \frac{1}{(1 - z \sin^2 x)^{1/2}} \quad (\text{A.6})$$

is the elliptic function of the first kind, while

$$E(z) = \int_0^{\pi/2} dx (1 - z \sin^2 x)^{1/2} \quad (\text{A.7})$$

is the elliptic function of the second kind.

- [1] Godrèche C and Bray A J, 2009 J. Stat. Mech. P12016
- [2] Godrèche C, 2011 J. Stat. Mech. P04005
- [3] Godrèche C, 2013 J. Stat. Mech. P05011
- [4] Glauber R G, 1963 J. Math. Phys. **4** 297
- [5] Kubo R, 1966 Rep. Prog. Phys. **29** 255
- Marconi U M B, Puglisi A, Rondoni L and Vulpiani A, 2008 Phys. Rep. **461** 111
- [6] Godrèche C and Luck J M, 2000 J. Phys. A **33** 1151
- [7] Lippiello E and Zannetti M 2000 Phys. Rev. E **61** 3369
- [8] Godrèche C and Luck J M, 2013 J. Stat. Mech. P05006
- [9] Godrèche C and Pleimling M, in preparation
- [10] Spitzer F, 1970 Advances in Math. **5** 246
- [11] Katz S, Lebowitz J L and Spohn H, 1983 Phys. Rev. B **28** 1655
- Katz S, Lebowitz J L and Spohn H, 1984 J. Stat. Phys. **34** 497
- [12] For reviews, see: Evans M R and Hanney T, 2005 J. Phys. A **38** R195
- Godrèche C, 2007 Lect. Notes Phys. **716** 261
- [13] Luck J M and Godrèche C, 2006 J. Stat. Mech. P08009
- [14] Künsch H R, 1984 Z. Wahrscheinlichkeitstheor. Verwandte. Geb. **66** 407
- [15] Godrèche C and Luck J M, 2002 J. Phys.: Condens. Matter **14** 1589
- [16] Calabrese P and Gambassi A, 2005 J. Phys. A **38** R133
- [17] For a review: Cugliandolo L F, 2011 J. Phys. A **44** 483001
- [18] Wang J S and Gan C K, 1998 Phys. Rev E **57** 6548
- [19] Mc Coy B and Wu T T, 1973 *The two-dimensional Ising model* (Cambridge: Harvard University Press)
- [20] Montroll E W, Potts R B and Ward J C, 1963 J. Math. Phys. **4** 308
- [21] Henkel M and Pleimling M, 2010 *Non-Equilibrium Phase Transitions 2: Ageing and Dynamical Scaling Far from equilibrium* (Dordrecht: Springer)
- [22] Barrat A, 1998 Phys. Rev. E **57** 3629
- [23] Manousiouthakis V I and Deem M W, 1999 J. Chem. Phys. **110** 2753
- [24] Ren R and Orkoulas G, 2006 J. Chem. Phys. **124** 064109
- [25] Suwa H and Todo S, 2010 Phys. Rev. Lett. **105** 120603
- [26] Turitsyn K S, Chertkov M and Vucelja M, 2011 Physica D **240** 410
- [27] Fernandes C M and Weigel M, 2011 Comp. Phys. Com. **182** 1856
- [28] Sakai Y and Hukushima K, 2013 J. Phys. Soc. Jpn. **82** 064003
- [29] Ichiki A and Ohzeki M, 2013 Phys. Rev. E **88** 020101(R)
- Ohzeki M and Ichiki A, 2013 arxiv/1307.0434